Potential of a PCM-Based Storage Concept Combined with an Electric Heat Pump

Anes Benzarti, Maximilian Hamilius, Stephan Roehrenbeck, Wolfram H. Wellssow
Chair for Energy Systems and Energy Management
TU Kaiserslautern
Germany
benzarti@eit.uni-kl.de

***Abstract*—This paper introduces a thermal storage concept for residential buildings based on a phase changing material (PCM). The proposed storage concept has been integrated in three different building classes equipped with an electric heat pump (EHP) and has been compared with a conventional thermal storage concept. The comparison has shown an improvement of the *SCOP* up to 13 %, depending on the heat demand of the building. Heating costs could be reduced about a fifth for all building types. Furthermore, a high flexibility can be made available when using PCMs with high phase changing enthalpy. These advantages are unfortunately accompanied with a small degradation in comfort, as sometimes the desired room temperature falls below the lower comfort boundary. This discomfort can be eliminated by adjusting the control scheme or by increasing the storage capacity. For grid operators this concept offers a huge flexibility potential on the demand side, as the hold-up time of heat pumps can be increased. For costumers the concept is attractive as the operational costs can be reduced.**

Keywords—electric heat pumps (EHP); distributed storage (DS); phase change materials (PCM); flexibility

NOMENCLATURE

This section defines the main symbols, abbreviations and indexes used in this paper. Others are defined as required in the text.

Symbols

A, B, R, F, M	Ambient air node, Building envelope node, Room air node, Floor heating layer node, heat transfer Material (e.g. water, PCM slurry) in the floor heating tubes node
A_F	Floor heating surface, in m²
c	Concentration of the PCM, in Vol–%
C	Thermal capacity, in J/K
C_j	Thermal capacity of the node j, in J/K
C_j'	Specific thermal capacity in node j, in J/m³·K
c_p	Specific heat capacity of the PCM, in J/kg·K
c_M	Specific heat capacity of the HTF (PCM slurry, water) in the tube, in J/kg·K
$c_{p,1}$, $c_{p,2}$	Specific heat capacity of the PCM in two states of aggregation (e.g. solid, liquid), in J/kg·K
COP	Coefficient of performance
d_{TB}	Distance between tube layer and building envelope, in m
d_B	Building envelope thickness, in m
d_t	Outer diameter of the tubes, in m
d_x	Distance between two tubes, in m
d_w	Thickness of the tube casing, in m
Δh	Phase change enthalpy of the PCM, in J/kg
l	Length of the tubes in the floor heating, in m
m	Mass of the PCM, in kg
$\dot{m}_M$	Mass flow of the HTF in the tubes, in kg/h
n_{op}	Number of operation times of the EHP during a heating period
$R_{ij}=R_{ji}$	Thermal resistance between node i and j, in K/W
R_z , R_w , R_r , R_x	Thermal resistances of the floor heating tube system, in K/W
t	Time step
T	Phase changing temperature of the PCM, in °C
T_j	Temperature of the node j, in °C
T_1 , T_2	Temperatures of the PCM in two states of aggregation (e.g. solid, liquid), in °C
T_2^{max}	Maximum allowed temperature for the RT22HC PCM, in °C
T_{min} , T_{max}	Minimum and maximum accepted temperatures in the PCM storage, in °C
Q_{min} , Q_{max}	Minimum and maximum SoC of the PCM storage, in J
Q_{pcm}	Thermal stored energy in a PCM during one cycle, in J
Q_{pcm}'	Thermal stored energy in 1 kg RT22HC in a temperature range of 14 °C and 29 °C, in kJ/kg
$\dot{Q}_{(\cdot)}^{gain}$, $\dot{Q}_{(\cdot)}^{loss}$	Thermal gains, Thermal losses, in W
$\dot{Q}_{j,t}$	Thermal gain in node j at time t, in W
SCOP	Seasonal coefficient of performance
V_R	Net air volume in the building, in m³
V_F	Net volume of the floor screed, in m³
λ, λ_B, λ_F	Specific thermal conductivity of the PCM, building wall and floor screed, in W/m·K
ρ	Density of the PCM, in kg/l

Abreviations

HTF	Heat transfer fluid
PCM	Phase change material
REF	Reference
SoC	State of charge
SFH	Single family house

This work is part of the project "Power to Heat for the Greater Region's Renewables Integration and Development" (PtH4GR²ID – 035-4-09-050) and has been financially supported by the European Regional Development Fund (EFRE) under the INTERREG V A–Greater Region program.

I. INTRODUCTION

Around 23 % of the yearly net energy consumption in Europe accounts for residential space heating and cooling [1]. In order to reduce the CO_2-emissions and fulfill the climate requirements of the European Union [2], a shift from fossil to renewable electrical heating, using e.g. the electric heat pump (EHP) technology, is inevitable. In Germany the share of heat pumps on the total heating systems is estimated to reach 26 % in 2030 compared to roughly 1 % in 2016 [3]. EHPs are a key technology and should be further developed in order to support the integration of renewables in low voltage (LV) grids. Different EHP control concepts have been proposed in the past [3–6]. However, all these concepts are delimited by the storage systems' characteristics to which the heating systems are connected. In fact, the used storage capacity is minor compared to the heating load of the building and is mainly dedicated to balance the mass flow and in particular cases to bypass an off-period defined by the power supply company. The thermal energy is stored in form of sensible heat in a hot water storage tank. This widespread thermal energy storage (TES) concept has three major drawbacks: low storage density, increasing losses with a higher state of charge (SoC) and a decreasing heat pump efficiency with a higher SoC. Nonetheless, this low-cost solution presents the state of the art for residential thermal appliances.

As flexibility on the demand side is gaining importance due to the high share of fluctuating renewable generation connected to the LV grid, alternative storage concepts are becoming attractive in order to provide the needed flexibility. Phase Change Materials (PCM) have a huge potential in this field as they have a much higher storage density than water and other sensible heat storage materials. Various research projects have been conducted in order to further develop PCM and make it competitive [9]. The available PCMs in the market cover a huge scope of temperatures, which can be used for different appliances.

Fig. 1 shows the PCM material classes which can be used for heating applications in residential buildings and their phase change enthalpy. Depending on the storage concept the needed phase change temperature can vary between the desired room comfort temperature and higher temperatures.

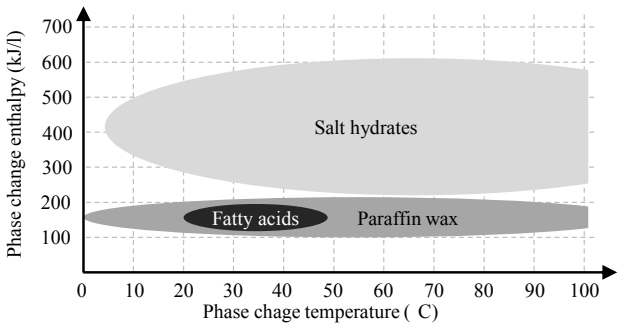

Figure 1. PCM classes for heating and cooling appliances in residential buildings, based on [10, 11]

II. STORAGE CONCEPT AND CHARACTERISTICS

A. Latent storage vs. sensible storage

Latent storage has the advantage of storing heat at a nearly constant temperature and thus reducing losses to a minimum. Furthermore, the storage capacity is usually higher than sensible storage [12]. Using PCM storage systems makes it possible to take advantage of both sensible and latent heat as shown in (1):

$$Q_{\text{pcm}} = \underbrace{m \cdot c_{p,1} \cdot \left(T - T_1\right) + m \cdot c_{p,2} \cdot \left(T_2 - T\right)}_{\text{sensible}} + \underbrace{\left(m \cdot \Delta h\right)}_{\text{latent}}. \quad (1)$$

B. Storage material

A paraffin wax has been chosen as PCM as it is cyclically stable and easy to handle compared to other PCMs. Furthermore, this material is non-toxic and non-corrosive [13]. The PCM is microencapsulated in order to prevent it from degradation and from mixing with the HTF when it is liquid. 40 % of the total TES volume is filled with PCM. The rest is filled with water as HTF. The combination of PCM capsules with HTF is called "PCM slurry". Tab. I shows the physical properties of the PCM used in the TES model.

TABLE I. PROPERTIES OF THE PARAFFINE PCM RT22HC [14]

c (Vol-%)	Q'_{pcm} (kJ/kg)	T (°C)	$T_2^{\max}$ (°C)	c_p (kJ/kg·K)	λ (W/m·K)	ρ (kg/l)	
						solid	*liquid*
40	190	22	50	2	0.2	0.76	0.70

C. Storage Concept

A concept has been adopted similar to the thermal activation of buildings using the building floor as a storage system [15]. Instead of using water as heat storage material, the above described PCM slurry has been integrated in a floor heating system model. No additional layers have been activated in order to keep both concepts comparable in terms of investment cost. Nevertheless, the storage capacity can be extended by activating the walls, too. Such a concept has not been investigated yet, because of fears that the temperature swings would be extreme and impair the thermal comfort in the building [15]. This thesis is discussed in section IV. Fig. 2 shows the arrangement of the tubes and the details of the combined heating and storage system.

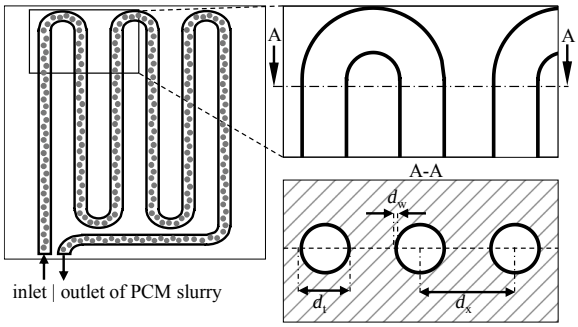

Figure 2. Scheme of a floor heating system equipped with PCM slurry as latent storage system

III. MODELS AND CONTROLS

In the following, two cases of simulations are distinguished requiring a number of models:

- A reference scenario composed of building models equipped with an EHP and a conventional TES, as described in Section I. This scenario is referred as "REF-case" in the following.
- A scenario where the PCM storage system, described in Section II, is modelled in combination with the same EHP and building models applied in the REF-case. This case is referred as "PCM-case".

Three building classes based on the TABULA classification [16] have been examined as shown in Tab. II.

TABLE II. CONSTRUCTION YEARS OF THE EXAMINED BUILDING CLASSES [16]

	SFH-E	SFH-H	SFH-K
Construction year	1958-1968	1984-1994	2010-2018

The simulations have been done for the climatic conditions corresponding to the climate zone 12 in Germany [17].

A. EHP model

An air to water fixed speed EHP has been chosen for the simulations. The EHP is equipped with an electrical auxiliary heating. The model is based on a curve fitting method and is described in previous work [3, 18, 19]. The same EHP model has been applied to both REF- and PCM-cases.

B. EHP control and storage management

1) REF-case: The EHP is equipped with a conventional thermostatic control. The heating curve as well as the hysteresis correspond to the assumptions made in [3] and [18]. The EHP switching mode depends on the storage temperature which is kept in a narrow band depending on the needed HTF temperature given by the heating curve.

2) PCM-case: The switching of the EHP (on), as well as the additional operation of the auxiliary heating (on$^+$) depend on the state of charge of the PCM storage and the ambient temperature T_A. When T_A is below 20 °C and the storage is discharged until a SoC of 10 %, the EHP is switched on and keeps operating until the SoC is at least 90 % or T_A becomes higher than 20 °C. The on/off mode between the lowest tolerable SoC of 10 % and the highest tolerable SoC of 90 % corresponds to a charging/discharging cycle. These limits have been set in order to delimit the temperature swings caused by sensible heat. In case the EHP power is not sufficient to meet the heat demand and the SoC reaches 0 % the auxiliary heating is switched on. When T_A is above 20 °C the heat pump is switched off independent of the SoC. The control scheme is illustrated in Fig. 3 for the selected temperature boundaries (T_{min}, T_{max}). The SoC of the PCM slurry storage is given in correlation with the aggregation state and the mean temperature in the storage for the PCM RT22HC.

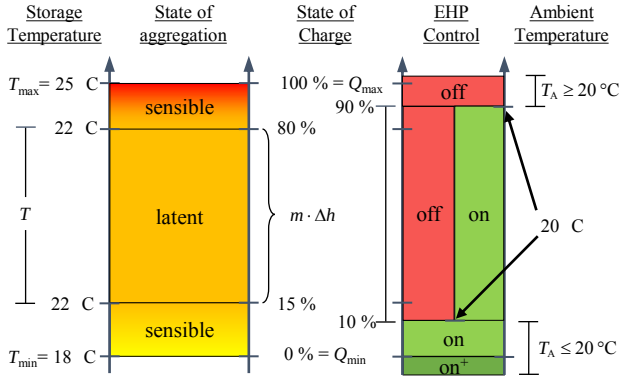

Figure 3. PCM storage behavior and control

Unlike the REF-case, which is equipped with a PID-control to regulate the mass flow in the heating system and hence the room temperature, this control scheme is not designed to keep the room temperature at a desired constant level, as no control of the mass flow has been foreseen. The objective here is to store the maximum of heat in the PCM slurry resulting in the maximum hold-up time of the EHP.

C. Building and storage models

In order to simulate the thermal behavior of the entire system a building model is needed. According to the literature, several models have already been developed using electrical analogies to reproduce the dynamic behavior of the buildings. The comparison of different models has shown, that the Laret 3R2C model is accurate enough [20–22].

As the storage system in the PCM-case is integrated in the floor heating system, as described in section II, the modeling of a combined heating and storage system is necessary. Therefore, the Laret model has been developed further. Fig. 4 shows an extended 3R2C model with three further resistances and an additional capacity, which has been applied for both the REF- and the PCM-case.

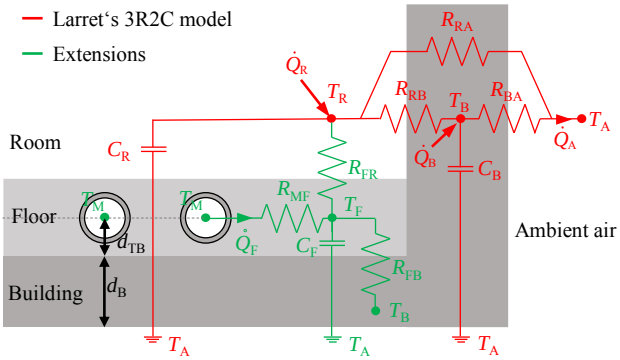

Figure 4. 6R3C Building and storage model overlaid with the physical system

The losses of the system can be determined based on the 6R3C model in Fig. 4:

$$\dot{Q}^{\text{loss}}_{\text{PCM-case}} = \dot{Q}^{\text{loss}}_{\text{A}} = \frac{T_{\text{B}} - T_{\text{A}}}{R_{\text{BA}}} + \frac{T_{\text{R}} - T_{\text{A}}}{R_{\text{RA}}} \,. \qquad (2)$$

For the PCM-case the storage system is integrated in the building and does not have any additional losses. However the storage system in the REF-case has additional losses, as heat water tanks are usually placed in the unheated cellar. In this scenario the most common storage type, a hot water buffer tank with a net volume of 667 l has been connected to the EHP. The mathematical formulation of the model is available from previous work [3, 18]. The losses in this case result in:

$$\dot{Q}^{\text{loss}}_{\text{REF-case}} = \dot{Q}^{\text{loss}}_{\text{A}} + \dot{Q}^{\text{loss}}_{\text{st}} . \qquad (3)$$

The above described model in Fig. 4 can be formulated as a differential equation system based on the dynamic behavior of the temperature $T_{j,t}$ at time t in the node j, $\forall\ j \in \{\text{B}, \text{R}, \text{F}\}$:

$$\begin{cases} C_{\mathrm{B}} \cdot \dfrac{\mathrm{d}\left(T_{\mathrm{B},t} - T_{\mathrm{A},t}\right)}{\mathrm{d}t} = \dot{Q}_{\mathrm{B},t} + \dfrac{T_{\mathrm{F},t} - T_{\mathrm{B},t}}{R_{\mathrm{FB}}} + \dfrac{T_{\mathrm{R},t} - T_{\mathrm{B},t}}{R_{\mathrm{RB}}} - \dfrac{T_{\mathrm{B},t} - T_{\mathrm{A},t}}{R_{\mathrm{BA}}}, & \text{(4a)} \\ C_{\mathrm{R}} \cdot \dfrac{\mathrm{d}\left(T_{\mathrm{R},t} - T_{\mathrm{A},t}\right)}{\mathrm{d}t} = \dot{Q}_{\mathrm{R},t} + \dfrac{T_{\mathrm{F},t} - T_{\mathrm{R},t}}{R_{\mathrm{FR}}} - \dfrac{T_{\mathrm{R},t} - T_{\mathrm{A},t}}{R_{\mathrm{RA}}} - \dfrac{T_{\mathrm{R},t} - T_{\mathrm{B},t}}{R_{\mathrm{RB}}}, & \text{(4b)} \\ C_{\mathrm{F}} \cdot \dfrac{\mathrm{d}\left(T_{\mathrm{F},t} - T_{\mathrm{A},t}\right)}{\mathrm{d}t} = \dfrac{T_{\mathrm{M},t} - T_{\mathrm{F},t}}{R_{\mathrm{MF}}} - \dfrac{T_{\mathrm{F},t} - T_{\mathrm{B},t}}{R_{\mathrm{FB}}} - \dfrac{T_{\mathrm{F},t} - T_{\mathrm{R},t}}{R_{\mathrm{FR}}}. & \text{(4c)} \end{cases}$$

The equation system (4) can be discretized and solved for each time step t. The temperatures T_{B}, T_{R} and T_{F} can be calculated at a time step t based on the ambient temperature T_{A}, the gains $\dot{Q}_{\mathrm{B}}$, $\dot{Q}_{\mathrm{R}}$ known for each time step and the temperatures T_{B}, T_{R}, T_{F} at the previous time step. T_{M} is calculated based on the outlet temperature of the heat pump and the current storage temperature.

This equation system can be simplified by assuming:

$$\forall\, i, j \in \{\mathrm{A},\mathrm{B},\mathrm{R},\mathrm{F},\mathrm{M}\};\quad \begin{cases} \theta_{ij,t} = T_{i,t} - T_{j,t}\,, & \text{(5a)} \\ \dot{\theta}_{j,t} = \dfrac{d\left(T_{j,t} - T_{\mathrm{A},t}\right)}{dt}\,, & \text{(5b)} \\ R_{ij} = R_{ji}\,, & \text{(5c)} \end{cases}$$

to obtain:

$$\begin{cases} C_{\mathrm{B}} \cdot \dot{\theta}_{\mathrm{B},t} = \dot{Q}_{\mathrm{B},t} + \dfrac{\theta_{\mathrm{FB},t}}{R_{\mathrm{FB}}} + \dfrac{\theta_{\mathrm{RB},t}}{R_{\mathrm{RB}}} + \dfrac{\theta_{\mathrm{AB},t}}{R_{\mathrm{AB}}}, & \text{(6a)} \\ C_{\mathrm{R}} \cdot \dot{\theta}_{\mathrm{R},t} = \dot{Q}_{\mathrm{R},t} + \dfrac{\theta_{\mathrm{FR},t}}{R_{\mathrm{FR}}} + \dfrac{\theta_{\mathrm{AR},t}}{R_{\mathrm{AR}}} + \dfrac{\theta_{\mathrm{BR},t}}{R_{\mathrm{BR}}}, & \text{(6b)} \\ C_{\mathrm{F}} \cdot \dot{\theta}_{\mathrm{F},t} = \dfrac{\theta_{\mathrm{MF},t}}{R_{\mathrm{MF},t}} + \dfrac{\theta_{\mathrm{BF},t}}{R_{\mathrm{BF}}} + \dfrac{\theta_{\mathrm{RF},t}}{R_{\mathrm{RF}}}. & \text{(6c)} \end{cases}$$

For all branches $\mathcal{B} = \{\mathrm{FB},\mathrm{RB},\mathrm{BA},\mathrm{RA},\mathrm{FM},\mathrm{FR}\}$ and nodes $\mathcal{N} = \{\mathrm{A},\mathrm{B},\mathrm{R},\mathrm{F},\mathrm{M}\}$ in the system, (6) can be expressed, as:

$$\forall\, j \in \{\mathrm{B},\mathrm{R},\mathrm{F}\}\,,\ \dot{\theta}_{j,t} = \frac{1}{c_j} \cdot \left(\dot{Q}_{j,t} + \sum_{\substack{i \in \mathcal{N} \\ i \neq j \\ ij,ji \in \mathcal{B}}} \frac{\theta_{ij,t}}{R_{ij,t}} \right). \qquad (7)$$

The thermal resistances related to the floor heating system can be expressed as in [23]:

$$\begin{cases} R_{\mathrm{FR}} = \dfrac{1}{A_{\mathrm{F}} \cdot 8.92 \cdot (\theta_{\mathrm{FR}})^{0.1}}\,, & \text{(8a)} \\ R_{\mathrm{FB}} = \dfrac{1}{3 \cdot A_{\mathrm{F}}} \cdot \left(\dfrac{d_{\mathrm{TB}}}{\lambda_{\mathrm{F}}} + \dfrac{d_{\mathrm{B}}/2}{\lambda_{\mathrm{B}}} \right), & \text{(8b)} \\ R_{\mathrm{MF}} = R_{\mathrm{z}} + R_{\mathrm{W}} + R_{\mathrm{r}} + R_{\mathrm{x}}\,. & \text{(8c)} \end{cases}$$

The time dependency of the resistances has been omitted for the sake of clarity. The tube resistance in (8c) can be expressed based on [23] by:

$$\begin{cases} R_{\mathrm{z}} = \dfrac{d_{\mathrm{x}} \cdot l}{2 \cdot \dot{m}_{\mathrm{M}} \cdot c_{\mathrm{M}}}\,, & \text{(9a)} \\ R_{\mathrm{r}} = \dfrac{d_{\mathrm{x}} \cdot \ln\left(\dfrac{d_{\mathrm{t}}}{d_{\mathrm{t}} - 2 \cdot d_{\mathrm{W}}} \right)}{2 \cdot \pi \cdot \lambda_{\mathrm{T}}}\,, & \text{(9b)} \\ R_{\mathrm{W}} = \dfrac{\left(d_{\mathrm{x}}\right)^{0.13}}{8 \cdot \pi} \cdot \left(\dfrac{\left(d_{\mathrm{t}} - 2d_{\mathrm{w}}\right) \cdot d_{\mathrm{x}}}{\dot{m}_{\mathrm{M}}} \right)^{0.87}, & \text{(9c)} \\ R_{\mathrm{x}} = \dfrac{d_{\mathrm{x}} \cdot \ln\left(\dfrac{d_{\mathrm{x}}}{\pi \cdot d_{\mathrm{t}}} \right)}{2 \cdot \pi \cdot \lambda_{\mathrm{F}}}\,. & \text{(9d)} \end{cases}$$

The thermal resistance between the building envelope and the ambient air has been determined based on the H'_{T} value. This value describes the conductivity of the entire building envelope and is calculated in [24] following the guidelines in [25]. The thermal resistance can be expressed as:

$$R_{\mathrm{BA}} = \frac{1}{H'_{\mathrm{T}}}\,. \qquad (10)$$

The thermal resistance between the room air and the building walls depends on the position of the wall and can be determined based on [26] as the sum of the specific resistances $R'_{\mathrm{RB},i}$ weighted with the respective areas $A_{\mathrm{R},i}$, as:

$$R_{\mathrm{RB}} = \sum_i \frac{R'_{\mathrm{RB},i}}{A_{\mathrm{R},i}}\,. \qquad (11)$$

Assuming that there is no mechanical ventilation in the residential building, the thermal resistance can be determined based on the air exchange rate in the building n_{x} [27]:

$$R_{\mathrm{RA}} = \frac{1}{\rho_A \cdot C_A \cdot n_{\mathrm{x}} \cdot V_{\mathrm{R}}}\,. \qquad (12)$$

The capacities are calculated, as:

$$\begin{cases} C_{\mathrm{B}} = C'_{\mathrm{B}} \cdot V_{\mathrm{R}}\,, & \text{(13a)} \\ C_{\mathrm{R}} = c_{\mathrm{p,A}} \cdot\ \rho_{\mathrm{A}} \cdot V_{\mathrm{R}}\,, & \text{(13b)} \\ C_{\mathrm{F}} = c_{\mathrm{p,F}} \cdot\ \rho_{\mathrm{F}} \cdot V_{\mathrm{F}}\,. & \text{(13c)} \end{cases}$$

IV. Simulation Results and Discussion

A. Efficiency of the EHP and the heating system

The comparison of the REF-case and PCM-case shows a difference in term of *SCOP*. This parameter is an indicator for the operational efficiency of the EHP during a whole heating period and is defined as:

$$SCOP = \frac{\sum_{i=1}^{n_{\mathrm{op}}} P_{\mathrm{el}}}{\sum_{i=1}^{n_{\mathrm{op}}} P_{\mathrm{th}}} = \frac{1}{n_{\mathrm{op}}} \cdot \sum_{i=1}^{n_{\mathrm{op}}} COP(i)\,. \qquad (14)$$

Fig. 5 shows the distribution of the *COP* values of the three modelled building classes during a heating period for both cases. The central mark in each box indicates the median of all values and the bottom and top edges of the box indicate the 25$^{\mathrm{th}}$ and 75$^{\mathrm{th}}$ percentile, respectively. The *SCOP* values are displayed using a '+' symbol.

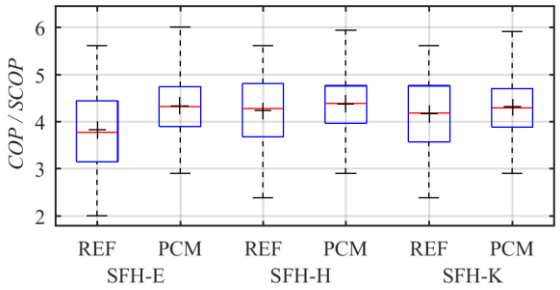

Figure 5. EHP operation efficiency for both cases in each building class

The *COP* depends on the ambient temperature T_A and on the temperature of the TES. As T_A is almost constant for both cases the different *COP* is mainly due to the different storage temperatures resulting from the difference in storage management. The storage temperature for the PCM-case is kept in a small band around the phase change temperature (approximately between 20 °C and 24 °C), while the storage temperature in the REF-case varies between approximately 35 °C and 65 °C depending on the ambient temperature.

The small deviation in the TES temperature for the PCM-case leads to a smaller deviation in the *COP* values compared to the REF-case. This can be observed from the distances between the bottom and top edges of the boxes for both cases. Furthermore, the influence of the TES temperature can be seen based on the lower whiskers (the lowest *COP* values in the box plots), which correspond to the lowest ambient temperature during the heating period. Those *COP* values remain constant for the PCM-case regardless of the building type, as the TES temperature is the same. For the REF-case the *COP* values increase with lower heat demand of the buildings (from building class E to K), which is due to the lower outlet temperature of the EHP and thus lower temperatures in the TES.

For the SFH-E the *SCOP* has been increased by 13 % when using the PCM based storage concept. This amelioration in the efficiency is due to the low operation temperature of the HTF, which is in average 18 K lower than in the REF-case. Both SFH-H and SFH-K show however a very slight amelioration. This is due to the low required HTF temperature for the floor heating even for the REF-case, as the buildings have respectively a 38 % and 65 % lower heat demand than the building SFH-E.

The *SCOP* is not sufficient to judge the efficiency of the heating system without taking the operation frequency of the EHP as well as the auxiliary heating into consideration. As the REF-case is equipped with a buffer storage, an additional heat sink is added to the energy balance equation, cf. (2) and (3). Therefore, the EHP is approximately 9.6 % more often in operation than in the PCM-case (e.g. SFH-H) in order to compensate these additional losses. This leads to a much lower efficiency of the whole system, in spite of the relatively high *SCOP*.

The whole system efficiency of the two cases is reflected in the operational expenditures (OPEX), assuming that only the electricity costs change from one case to the other. This difference in *OPEX* corresponds to the savings due to the PCM storage concept. Table III shows the *OPEX* ratios of the two cases.

TABLE III. OPERATIONAL EXPENDITURE RATIO FOR EACH BUILDING CLASS

$\frac{OPEX_{PCM}}{OPEX_{REF}}$	SFH-E	SFH-H	SFH-K
	0.79	0.79	0.78

It can be concluded that approximately one fifth of the operational costs can be saved regardless the building class.

B. *Comfort in the building*

One of the comfort factors is the average air temperature in the building T_R, which should be kept close to the target room temperature T_{tar}. Fig. 6 shows the distribution of T_R for both cases for the building class SFH-H with a target room temperature $T_{tar} = 20$ °C.

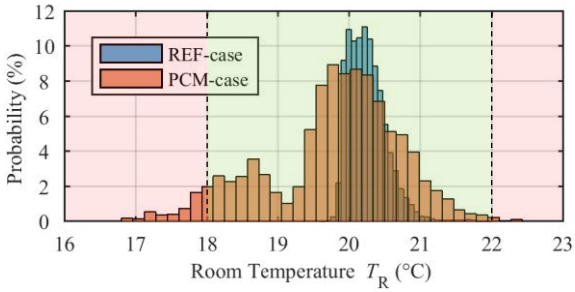

Figure 6. Distribution of the room temperature in SFH-H during a heating period for both examined cases

A clear drawback of the proposed PCM storage control is the comfort loss. The room temperature T_R cannot be kept constant at T_{tar} as expected in section III. Assuming a tolerable deviation of $\Delta T_{tol} = \pm 2$ °C from the target room temperature $T_{tar} = 20$ °C, T_R can vary between 18 °C and 22 °C without any considerable loss of comfort. A limit violation in 3 % of the time steps for the building type SFH-H is observed. For the building classes SFH-E and SFH-K, 11 % and 0.8 % of the T_R values are respectively beyond these boundaries. The discomfort obviously increases with a higher heat demand of the building which is clearly due to the insufficient dimensioning of the storage system. During extreme weather conditions ($T_A < -5$ °C) the heat demand of the buildings cannot be covered for any of the building classes and the room temperature drops below the lower comfort limit of 18 °C. Nevertheless, the deviation from this target temperature remains almost acceptable for building classes with low heat demand (c.f. SFH-K). In order to fulfill the comfort requirements the storage capacity has to be increased, either by using a PCM with higher phase changing enthalpy or by activating the walls of the building. An increase in storage capacity doesn't influence the *SCOP* for the PCM-case as the average storage temperature remains unchanged.

C. *Flexibility and hold-up time*

Flexibility can be defined as the capability of the EHP operation to deviate from the required heat demand of the building. The amount of flexibility is directly connected to the storage capacity as well as the heat demand of the building, which depends on the weather conditions. An indicator of flexibility is the hold-up time or the must-run time of the EHP when the storage system is fully loaded or empty, respectively. Fig. 7 shows the hold-up time dependency from the ambient temperature for the REF-case and PCM-case with different phase change enthalpies, examined for the building class SFH-H.

The hold-up time reflects the storage capacity of the different cases. With the commercially available PCM from Tab. I (referred as "PCM-case (Δh)" in Fig. 7) integrated in the floor heating without any additional activation of further surfaces in the building, no gain in flexibility can be achieved compared to the REF-case. The storage capacity in this PCM-case is even lower compared to the REF-case.

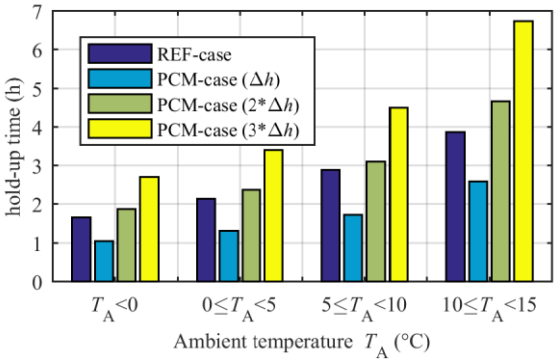

Figure 7. Flexibility on the consumer side depending on the ambient temperature

The hold-up time depends strongly on the ambient temperature. A ratio of 2 can be noticed when comparing the hold-up time for ambient temperatures 0 °C<T_A<5 °C and 10 °C<T_A<15 °C. For ambient temperatures higher than 10 °C a hold-up time higher than 2 h can be achieved in all four cases.

By applying other PCMs with doubled or tripled phase change enthalpy (2*Δh, 3*Δh) the flexibility can be increased to an average value higher than 2 h even for ambient temperatures below 0 °C. Nevertheless, the hold-up time cannot be doubled by doubling Δh as the sensible part of the storage capacity remains unchanged. As the used PCM in the storage model has a relatively low phase change enthalpy compared to other PCMs like salt hydrates (cf. Fig. 1) the flexibility potential can be easily increased by applying other materials.

Furthermore, the activation of additional walls in the building is an option if investment costs doesn't matter. This would lead to a much higher storage capacity. Doubling the storage volume will double the flexibility.

V. Conclusion

The proposed PCM storage concept shows several advantages and has a huge saving potential from an energetic and economic point of view. The efficiency of the entire heating system can be increased, regardless of the building class, even in case of a low storage capacity.

This paper shows that the application of other PCM materials with higher storage density, having melting temperatures around the desired comfort temperature, would improve the flexibility on the demand side as the storage capacity would be higher. This would allow to support the LV-grid, to contribute to the active power balancing and to apply advanced EHP control schemes. Furthermore, the concept of core activation can be applied and additional walls can be activated in order to increase the storage capacity and hence the flexibility. This will be further analyzed in future work together with a profitability analysis in terms of net present values.

As the objective of this paper is the analysis of storage concepts and their benefits, the control scheme was not the main focus, leading to a clear discomfort compared to a conventional heating system. The temperature swings increase with higher heat demand of the building. Higher storage capacities and a more sophisticated control scheme would enhance the comfort in the building. This would lead to an even higher flexibility on the demand side.

References

[1] "COMMISSION STAFF WORKING DOCUMENT Review of available information Accompanying the document Communication from the Commission to the European Parliament, the Council, the European Economic and Social Committee and the Committee of the Regions on an EU Strategy for Heating and Cooling," in EUR-Lex, 2016.

[2] "Directive 2009/28/EC of the European Parliament and of the Council of 23 April 2009 on the promotion of the use of energy from renewable sources and amending and subsequently repealing Directives 2001/77/EC and 2003/30/EC: L 140/16," in EUR-Lex, 2009.

[3] S. Röhrenbeck et al., "Prädiktive Betriebsoptimierung drehzahlvariabler Wärmepumpen in Kombination mit preisvariablen Stromtarifen," in Internet der Dinge: VDE-Kongress 2016 Mannheim, 7. und 8. November 2016, V. d. E. E. I. e. V. (VDE), Ed., 2016.

[4] M. U. Kajgaard, J. Mogensen, A. Wittendorff, A. T. Veress, and B. Biegel, Eds., Model predictive control of domestic heat pump. 2013 American Control Conference, 2013.

[5] M. Loesch, D. Hufnagel, S. Steuer, T. Faßnacht, and H. Schmeck, Eds., Demand side management in smart buildings by intelligent scheduling of heat pumps. 2014 IEEE International Conference on Intelligent Energy and Power Systems (IEPS), 2014.

[6] G. Masy, E. Georges, C. Verhelst, V. Lemort, and P. André, "Smart grid energy flexible buildings through the use of heat pumps and building thermal mass as energy storage in the Belgian context," (en), Science and Technology for the Built Environment, vol. 21, 2015.

[7] M. A. Lambert, "Design of solar powered adsorption heat pump with ice storage," (en), Applied Thermal Engineering, vol. 27, no. 8, pp. 1612–1628, 2007.

[8] T. Faßnacht, M. Loesch, and A. Wagner, "Simulation study of a heuristic predictive optimization scheme for grid-reactive heat pump operation," in Proceedings of REHVA Annual Conference 2015 "Advanced HVAC and Natural Gas Technologies", pp. 132–141.

[9] M. Kenisarin and K. Mahkamov, "Salt hydrates as latent heat storage materials: Thermophysical properties and costs," (en), 2016.

[10] BINE Informationsdienst, Latentwärmespeicher in Gebäuden - Phasenübergang puffert Wärme II. [Online] Available: http://www.bine.info/publikationen/themeninfos/publikation/latentwaermespeicher-in-gebaeuden/phasenuebergang-puffert-waerme-forts/.

[11] J. H. Dieckmann, "Latent heat storage in concrete," (af), 2006.

[12] T. Bauer, W.-D. Steinmann, D. Laing, and R. Tamme, "Thermal Energy Storage Materials and Systems: Chapter 5. Annual Review of Heat Transfer," (en), pp. 131–177.

[13] S. Blankenburg, Ed., Workshop Wärmespeicherung, 2001.

[14] Rubitherm GmbH, "Technisches Datenblatt: RT22HC,"

[15] B. W. Olesen, "Thermo Active Building Systems Using Building Mass To Heat and Cool," (en), A S H R A E Journal, no. 54, pp. 44–52, 2012.

[16] Deutsche Wohngebäudetypologie: Beispielhafte Maßnahmen zur Verbesserung der Energieeffizienz von typischen Wohngebäuden. Darmstadt: Wohnen und Umwelt, 2015.

[17] Bundesamtes für Bauwesen und Raumordnung (BBR), Ed., "Ortsgenaue Testreferenzjahre von Deutschland für mittlere, extreme und zukünftige Witterungsverhältnisse," Deutscher Wetterdienst (DWD), Jul. 2017.

[18] S. Röhrenbeck et al., "Assisting Renewable Energy Integration by Price Based Load Shifting using Heat Pumps with Thermal Storage," in Die Energiewende - Blueprint for the new energy age: ETG Congress 2017 Bonn, 28. und 29. November 2017, V. d. E. E. I. e. V. (VDE), Ed., 2017.

[19] W. H. Wellßow et al., “ThermSpe4EE : EE-Integration durch stromgeführte Wärmepumpen, Nutzung der Bestandsgebäude als Energiespeicher, Einsatz zusätzlicher thermischer Speicher und Anwendung zeitvariabler Tarife : Schlussbericht - Teilbericht TUK : Laufzeit: 01.11.2014 bis 31.08.2017,” Technische Universität Kaiserslautern, Kaiserslautern 0325730B. 01154283, 2018.

[20] Samuel F. Fux, Araz Ashouri, Michael J. Benz, and Lino Guzzella, “EKF based self-adaptive thermal model for a passive house,” (ca), Energy and Buildings, vol. 68, pp. 811–817, http://www.sciencedirect.com/science/article/pii/S0378778812003039, 2014.

[21] T. Faßnacht, H. Östreicher, and A. Wagner, Gebäudemodelle für modellbasierte Regler und Energiemanagementsysteme (de).

[22] V.S.K.V. Harish and Arun Kumar, “A review on modeling and simulation of building energy systems,” (en), Renewable and Sustainable Energy Reviews, vol. 56, pp. 1272–1292, http://www.sciencedirect.com/science/article/pii/S1364032115014239, 2016.

[23] M. Koschenz and B. Lehman, Thermoaktive Bauteilsysteme tabs, 1st ed. Dübendorf: EMPA Energiesysteme/Haustechnik, 2000.

[24] Institut Wohnen und Umwelt, Thermal Insulation Measures: Calculation PDF 1. Typology Approach for Building Stock Energy Assessment. [Online] Available: http://webtool.building-typology.eu. Accessed on: 19/13/2018.

[25] Thermal performance of buildings – Transmission and ventilation heat transfer coefficients – Calculation method (ISO 13789:2007), 2008.

[26] Building components and building elements – Thermal resistance and thermal transmittance – Calculation methods (ISO 6946:2017); German version EN ISO 6946:2017, 2018.

[27] Thermal protection and energy economy in buildings — Part 6: Calculation of annual heat and annual energy use, 4180-6, 2003.